

Silicon Microstrip Detectors for the CMS experiment at LHC

C. Civinini^a

^aINFN sez. di Firenze, Lgo. E. Fermi 2, I-50125 Firenze, Italy
CMS Collaboration

During the last few years a large number of Silicon Microstrip Detectors have been especially designed and tested by the CMS collaboration in order to study and optimize the performances of the tracking devices to be used in the inner part of the experiment.

Both single and double sided silicon detectors of different shapes and strips configuration, including prototypes produced with double metal technology, have been exposed to high energy beams. The main results on detector performances (charge response, signal to noise ratio, spatial resolution etc.) will be reviewed and discussed.

1. Introduction

The proposed CMS silicon tracker [1] is made of four layers of silicon microstrip detectors instrumenting the intermediate part of the tracking cavity, between the inner pixel detector and the outer MSGC layers. For a layout of the CMS tracker see ref. [2]. These sets of high precision position sensitive detectors will provide the measurements of the charged particle momentum by accurate determination of its trajectory in the CMS solenoidal magnetic field. This paper will describe some of the silicon microstrip detectors that have been designed and tested in the R&D effort that aims at the final definition of the tracker.

The CMS silicon tracker can be subdivided in two different regions: central (or “barrel”) and forward. In the barrel region, rectangular detectors with p-strips oriented along the beam direction are expected to provide point resolution better than $15\ \mu\text{m}$ in the bending plane for perpendicular incidence; a coarse measurement ($\sigma \simeq 1\ \text{mm}$) of the coordinate along the beam is obtained by double-sided detectors with stereo strips on the n-side. Similarly, in the forward-backward regions wedge-shaped detectors will provide precise measurements of the azimuthal coordinate and a coarse measurement of the radial position. Four basic types of silicon detectors are therefore included in the baseline layout: single and double-sided devices (SS or DS

respectively), in two different geometries (rectangular and wedge). These detectors, and other R&D devices, have been tested in high energy particle beams using fast electronics (PreMux128 [3]) similar to the final chip [4] foreseen for LHC; the performances in terms of signal-to-noise ratio and space resolution will be shown to be compatible with the design parameters contained in the CMS Technical Proposal.

2. Detectors

All detectors were built from standard n-type high resistivity silicon wafers, $300\ \mu\text{m}$ thick [5–7]. All single- and double-sided microstrip detectors tested have identical structures on the p-side. Each strip is AC coupled to external amplifiers by means of integrated capacitors built on the wafer itself. Bias is provided to the strips via polysilicon resistors connected to the guard-ring structure. A similar arrangement is used on the n-side of the double-sided devices with the addition of an isolation p-stop implant box surrounding each electrode. In the devices featuring what we will call in the following “Double-Metal technology” (DM) the n-side electrodes are connected, through a small contact, with a metal fan-out deposited on top of a thick insulator layer.

The single-sided full size barrel prototype (SSFS) is made of two detectors glued together with the strips daisy chained for a total length of $124.4\ \text{mm}$; the strip pitch is $50\ \mu\text{m}$. The so-called

stereo detectors are double-sided devices where the strips on the n-side are tilted at an angle, in our case 100 mrad, with respect to those on the p-side. Fig. 1 shows the layout of the n-side strips for the DS Stereo DM detectors (DSSDM), a prototype of the devices to be used in the barrel part of the tracker. In this case the DM technology al-

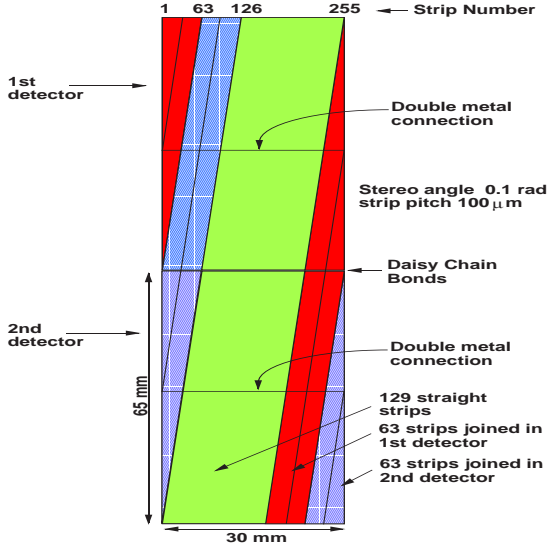


Figure 1. Schematic description of two DSSDM detectors assembled in a module (n-side view). Double Metal connections that joins different strips across the detector are shown.

lows to design the stereo n-side eliminating the dead regions that usually affect this kind of detectors. The strip pitch is $50 \mu\text{m}$ for the p-side and $100 \mu\text{m}$ for the n-side. One of this detectors has been assembled connecting to the electronics only one n-side strip out of two; in such a way the corresponding read-out pitch becomes $200 \mu\text{m}$.

Another double-sided detector that makes use of the DM technology is the DSODM. This detector is similar to the DSSDM except the orientation of the n-side strips that in this case are orthogonal to the p-side ones and are all connected to the electronics at $100 \mu\text{m}$ pitch.

For the Wedge detector [8,9] (fig. 2) the strips of the p-side (62 mm long) follow a trapezoidal geometry with a corresponding pitch changing from 38 to $50 \mu\text{m}$. The n-side strips (length between

4.8 mm and 6.3 mm) have a pitch of $125 \mu\text{m}$ and are orthogonal to the central strip of the p-side. This is a R&D device designed to understand the performances of a variable pitch detector, very similar to the ones to be used in the forward part of the tracker.

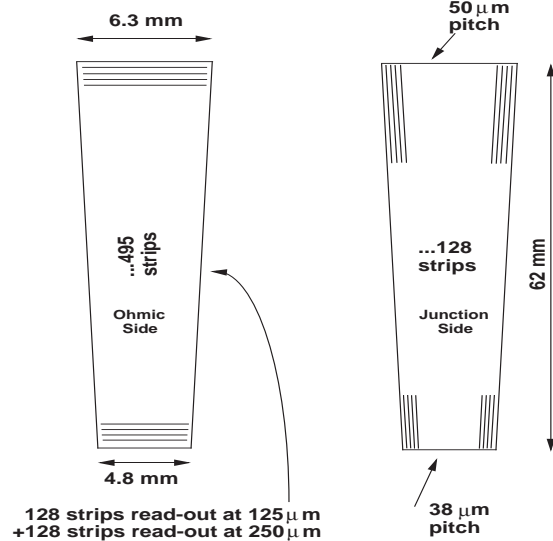


Figure 2. Wedge detector schematic description.

Other detectors that have been realized in the framework of this R&D programme, but whose results are extensively discussed elsewhere [10], are: a double-sided detector with the n-side segmented with pads; a small size double-sided detector where a read-out pitch of $50 \mu\text{m}$ is used for the n-side too; and a single-sided small size detector (SS) read-out with slower electronics.

3. Tests Beam

The results presented in this paper comes from data taken in a series of beam tests done at CERN during the years 1995 and 1996.

3.1. Read-out Electronics

Apart some detector read-out with slow electronics (VA1) or fast chips without multiplexing capabilities (PreShape32 [11]), all data were taken using a fast (45 ns nominal shaping time) chip (PreMux128) designed to match the LHC requirements.

3.2. Test Beam configuration

The tests were done using two different extracted SPS beams at North (H2 beam) and West (X7 beam) SPS experimental halls.

Description of H2 test area can be found in ref.[13]. Several detectors, grouped as B_1 , B_2 and H_1 , were used as reference telescopes to precisely reconstruct the trajectories of incoming particles.

B_1 and B_2 each consisted of two identical double-sided silicon microstrip detectors with orthogonal strips. The spatial resolution [12], was $3 \mu\text{m}$ on the p-side and $6 \mu\text{m}$ on the n-side. H_1 was made of eight single-sided silicon detectors with a spatial resolution of $6 \mu\text{m}$ for each plane.

For the test done in X7 one more telescope with bigger active area (B_3) was added.

In both tests the detectors were mounted on frames that allowed for rotation around a horizontal axis perpendicular to the beam and placed between the telescopes for the determination of the position resolution.

3.3. Data Acquisition System

During the H2 beam test the data acquisition was based on the RD5 framework.

Those detectors that were equipped with VA1 chips, as well as the B1 and B2 telescopes, were read out using a VME Flash ADC (SIROCCO-1 [14]). The FADC boards were controlled and read out by MC68020 cards, and the data transferred over to the event builder crate using Dual Port Memories (DPM) for logging and monitoring.

For the X7 test almost all detectors, which were by then equipped with PreMux128 electronics, were read out by either SIROCCO-1 or CAEN V551 FADC boards.

The Wedge and DSODM read out system [15] used different ADCs and an extensive decoupling scheme allowing a fully floating connection to the detectors. The data coming from the ADCs were transferred to a VME crate and written, under the control of Motorola CPU's, into a DPM which interfaced the system to the main DAQ.

The rest of the multi-crate system was controlled by MC68040 processors in the front-end crates and a Sparc 5/64 processor was used for tape writing and monitoring.

4. Results

In the following some of the most significant results obtained during these tests beam will be shown. The purpose of the test activity described in this paper was to check carefully the performances of non-irradiated detectors in terms of signal to noise ratio and space resolution under different conditions of bias voltage and for tracks at various incidence angle.

4.1. Offline Analysis

The signal $S^{(i)}$ on the i -th strip at each event is extracted from the value read from the analog-to-digital converter, $ADC^{(i)}$, by subtracting the strip pedestal $PED^{(i)}$ and the common mode fluctuation for the event, CM :

$$S^{(i)} = ADC^{(i)} - PED^{(i)} - CM.$$

Two different algorithms to extract the pedestal, the common mode and the noise values ($N^{(i)}$) have been developed; both methods give comparable results.

Once $S^{(i)}$ and $N^{(i)}$ have been calculated from the raw data an algorithm is applied to look for clusters of adjacent strips in order to identify the passage of a particle through the detector. The cluster noise is then defined as $N^{cluster} = \sqrt{\sum_{cluster} [N^{(i)}]^2 / L^{cluster}}$, where $L^{cluster}$ is the number of strips accepted for that cluster. Typical ranges for the cut values used by this algorithm to identify a cluster are: $S^{(i)}/N^{(i)} > 3 \div 5$ for the cluster "seed", $S^{(i)}/N^{(i)} > 2$ for cluster lateral strips and finally $S^{cluster}/N^{cluster} > 5 \div 10$ for the total cluster signal.

To determine the spatial resolution of the detectors we used the tracking information provided by the beam telescopes. For this purpose, all the system must be properly aligned first. This procedure computes, for each detector, the three translational offsets in x , y and z and the rotation angle ϕ in the plane orthogonal to the nominal beam direction; the other possible rotations were found to give negligible effects. These parameters are computed minimizing the width of the residual distributions (differences between the locally reconstructed point and the computed intersection of the extrapolated track and the detector). Two

different alignment procedures have been developed, both giving consistent results.

4.2. Charge Response and Signal to Noise Ratio

The response of a detector to the charge released in the silicon by an ionizing particle is given by $S^{cluster}$. A typical distribution of this quantity is shown in fig. 3.

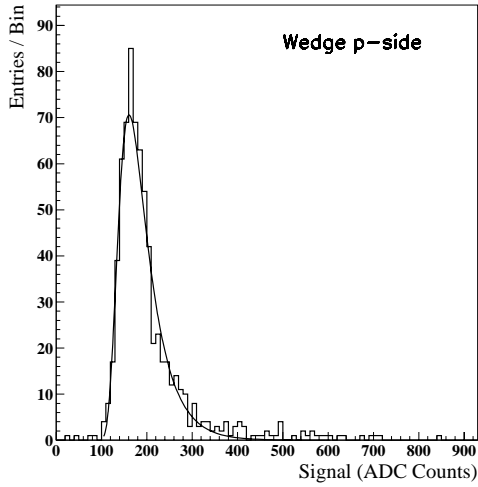


Figure 3. Charge response of the Wedge detector (bias 100 V, normal incidence). A fit with a Landau function is superimposed.

A summary of the signal-to-noise performances for different detectors is shown in table 1. The figures listed are computed as the ratio of the most probable cluster signal value from the Landau fit to the average noise as fitted with a Gaussian.

4.3. Bias and Angular Scan

On all devices we performed a voltage scan to study the effect of different bias voltages on the signal-to-noise ratio (see for example fig. 4). A slight improvement of the signal-to-noise ratio even after full depletion (~ 40 Volts) can be seen in figg. 4b and c.

This effect may be an indication of a better charge collection efficiency due to the higher electric field inside the silicon when detectors are read-out with fast electronics.

| | | Signal / Noise | | | | | |
|---|--|----------------|------|-------|-------|------|-------|
| | | SS | SSFS | DSODM | DSSDM | | Wedge |
| | | | | | 100 | 200 | |
| p | | 27. | 26.1 | 23.2 | 14.9 | 13.4 | 26.5 |
| n | | - | - | 17. | 8.4 | 11. | 38.4* |

Table 1

Signal to noise ratio for detectors tested at nominal conditions. The figure marked with an asterisk was obtained averaging the results from separate distributions for single- and multi-strip clusters.

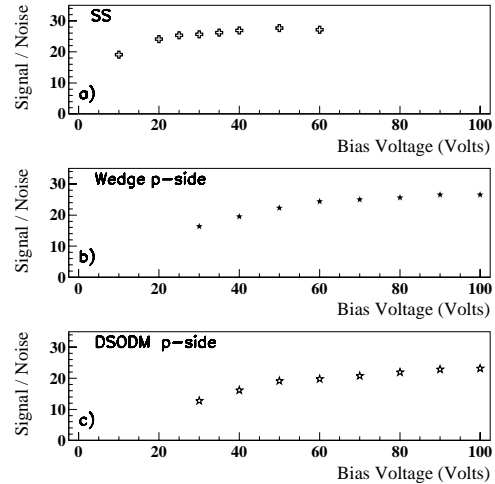


Figure 4. Signal to Noise ratio versus the applied voltage for: a) SS, b) Wedge p-side, c) DSODM p-side.

All data presented so far were taken exposing the detectors to the beam at normal incidence. The effect of inclined tracks on the response of the p-side has been studied in detail by rotating the detector modules around the horizontal axis perpendicular to the beam direction.

The detectors were mounted with the p-side strips parallel to the rotation axis, therefore the amount of charge released in the silicon and the cluster width are expected to increase for geometrical reasons.

Examples of the behaviour of the various parameters are shown in fig. 5 for the p-side of DSODM.

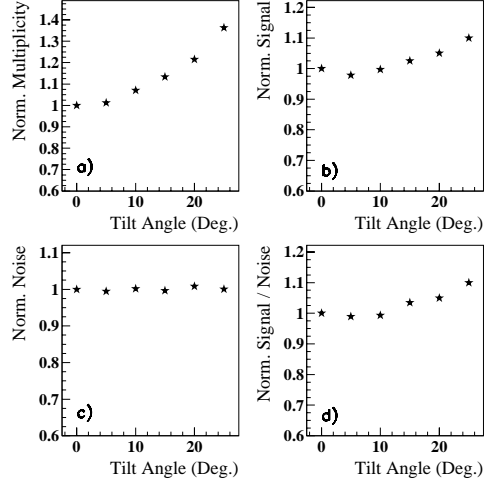


Figure 5. Scan in the tilt angle for the p-side of a DSODM detector; all points are normalized to the orthogonal incidence values: a) Mean number of strips in cluster, b) Most probable cluster signal, c) Mean cluster noise, d) Signal to noise ratio.

4.4. Spatial Resolution

The detectors were placed within a high precision telescope system to study the position resolution. To reconstruct the particle impact point from the cluster information, the center of gravity of the cluster, using as weight the charge collected on each strip, was evaluated. A typical distribution of the residual, computed using the telescope information to extrapolate the particle track on the detector plane, is plotted in fig. 6 for the Wedge detector. By subtracting in quadrature the telescope tracking error from the width of the residual distributions we obtain the resolution values listed in table 2.

In the CMS baseline Tracker, the stereo strips are used to measure the so-called “secondary” coordinate, perpendicular to the high-precision one measured by the p-side strips, through the association between hits on the two views.

The resolution in the intrinsic coordinate for the two stereo detectors (DSSDM₁₀₀ and DSSDM₂₀₀) has been evaluated from the distribution of residuals shown in fig. 7a and c. The

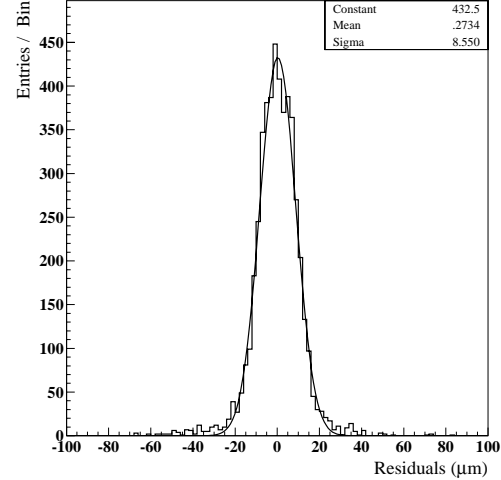


Figure 6. Residuals for the p-side of Wedge detector.

| | | Resolution (μm) | | | | | |
|---|--|------------------------------|------|-------|------------------|------------------|-------|
| | | SS | SSFS | DSODM | DSSDM | | Wedge |
| | | | | | 100 | 200 | |
| p | | 12 | 11 | 11 | 12 | 12 | 7 |
| n | | - | - | 17 | 325 ^a | 357 ^a | 23 |
| | | | | | 32 ^b | 35 ^b | |

Table 2

Spatial resolution in μm for all tested detectors. Superscript a) refers to the resolution in the secondary coordinate (orthogonal to the one measured by the p-side), while b) refers to the resolution in the intrinsic n-side coordinate.

widths of the two distributions are comparable: $34 \mu\text{m}$ vs $36 \mu\text{m}$ as expected as a consequence of the presence of the floating strips in the $200 \mu\text{m}$ read-out pitch detector (DSSDM₂₀₀). The resolution in the secondary coordinate is shown in fig. 7b and d: the widths of the two distributions are respectively $327 \mu\text{m}$ and $357 \mu\text{m}$. From these values, obtained with a stereo angle of 100 mrad , we can extrapolate a resolution for the baseline CMS Double-Sided Stereo Module ($200 \mu\text{m}$ read-out pitch, floating strip and a stereo angle of 60 mrad) of about $600 \mu\text{m}$, well within the expected requirements.

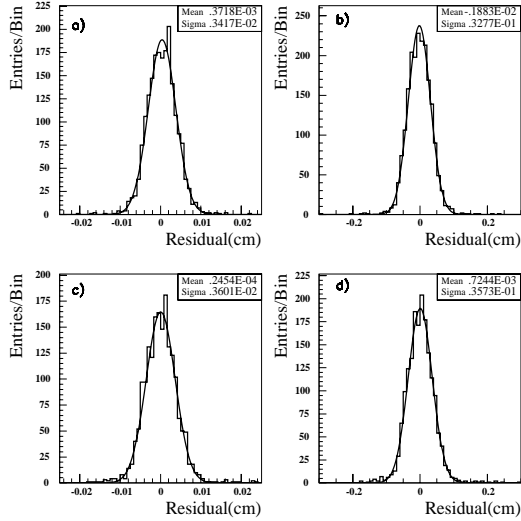


Figure 7. Residuals for the n-side of DSSDM detectors: **a)** intrinsic coordinate for DSSDM₁₀₀; **b)** secondary coordinate for DSSDM₁₀₀; **c)** intrinsic coordinate for DSSDM₂₀₀; **d)** secondary coordinate for DSSDM₂₀₀.

5. Conclusions

In the framework of the R&D programme aimed at the design and optimization of the CMS Silicon Tracker several silicon microstrips detectors have been realized and tested.

The measured resolution of all tested detectors is well within the requirements set for the CMS Silicon Tracker. The signal to noise ratio measured on a full size prototype is quite satisfactory (26:1); anyway we expect a worsening of this figure due to the use of the final front-end chip (factor 1.4) and a degradation of the detector because of the radiation damage. Nevertheless we still have a large margin before reaching an average signal to noise ratio of 10:1, which is considered our lower limit for safe operation after 10 years of high-luminosity operation at the LHC.

Acknowledgments

This paper is based on the material contained in several CMS documents and technical notes. I

would like to thank all my colleagues who contributed to the works from which I have drawn this material.

REFERENCES

1. The Compact Muon Solenoid, "Technical Proposal", CERN/LHCC 94-38 LHCC/P1, 15 December 1994.
2. R. Ribeiro, "The CMS central tracker", these proceedings.
3. L. L. Jones, "*PreMux128 User Manual*."
4. M. French et al., CERN/LHCC/95-56.
5. P. Weiss et al., "*Wafer-Scale Technology for Double-Sided Silicon Microstrip Particle Detectors*", The 7th International Conference on Solid-State Sensors and Actuators.
6. G. Tonelli et al., Nucl. Instrum. and Meth. A377 (1996) 422.
7. A. Holmes-Siedle et al., NIM A339 (1994) 511.
8. E. Catacchini et al. "*Wedge silicon detectors for the inner tracking system of CMS*", 6th Topical Seminar on "Experimental Apparatus for Particle Physics and Astrophysics", S.Miniato 1996.
9. E. Catacchini, "*Characterization of a Double Sided Microstrip Silicon Wedge Detector*", these proceedings.
10. O. Adriani et. al., "*Beam Test Results for Single- and Double-Sided Silicon Detector Prototypes of the CMS Central Detector*", CMS Note 1997/006.
11. M. Raymond and L. Jones, "*RD20 Pre-Shape32 User Manual*."
12. L. Celano et al., "*A High Resolution Beam Telescope Built with Double Sided silicon Strip Detectors*", accepted for publication by NIM
13. RD5 Collaboration, "*Status Report of the RD5 Experiment*", CERN/DRDC 93-49.
14. W. Dulinski et al., "*VME Flash ADC multi-purpose module*", Draft, VFLAM-CRN/Lepsi 1992.
15. O. Adriani et al., "*A data acquisition system for silicon microstrip detectors*", Dipartimento di Fisica e INFN Firenze Preprint DFF 237/11/95.